



# The effect of flow modes and electrode combinations on the performance of a multiple module microbial fuel cell installed at wastewater treatment plant

Weihua He<sup>a</sup>, Maxwell J. Wallack<sup>b</sup>, Kyoung-Yeol Kim<sup>b</sup>, Xiaoyuan Zhang<sup>b,c</sup>, Wulin Yang<sup>b</sup>, Xiuping Zhu<sup>b,d</sup>, Yujie Feng<sup>a,\*</sup>, Bruce E. Logan<sup>a,b,\*</sup>

<sup>a</sup> State Key Laboratory of Urban Water Resource and Environment, Harbin Institute of Technology, No. 73 Huanghe Road, Nangang District, Harbin 150090, PR China

<sup>b</sup> Department of Civil & Environmental Engineering, Penn State University, 231Q Sackett Building, University Park, PA 16802, USA

<sup>c</sup> State Key Joint Laboratory of Environment Simulation and Pollution Control, School of Environment, Tsinghua University, Beijing 100084, PR China

<sup>d</sup> Department of Civil & Environmental Engineering, Louisiana State University, Baton Rouge, LA 16802, USA

## ARTICLE INFO

### Article history:

Received 21 March 2016

Received in revised form

4 September 2016

Accepted 6 September 2016

Available online 9 September 2016

### Keywords:

Microbial fuel cell

Alternating flow

Multi-module reactor

Electrode combinations

Domestic wastewater treatment

## ABSTRACT

A larger (6.1 L) MFC stack made in a scalable configuration was constructed with four anode modules and three (two-sided) cathode modules, and tested at a wastewater treatment plant for performance in terms of chemical oxygen demand (COD) removal and power generation. Domestic wastewater was fed either in parallel (raw wastewater to each individual anode module) or series (sequentially through the chambers), with the flow direction either alternated every one or two days or kept fixed in a single direction over time. The largest impact on performance was the wastewater COD concentration, which greatly impacted power production, but did not affect the percentage of COD removal. With higher COD concentrations ( $\sim 500 \text{ mg L}^{-1}$ ) and alternating flow conditions, power generation was primarily limited by the cathode specific area. In alternating flow operation, anode modules connected to two cathodes produced an average maximum power density of  $6.0 \pm 0.4 \text{ W m}^{-3}$ , which was  $1.9 \pm 0.2$  times that obtained for anodes connected to a single cathode. In fixed flow operation, a large subsequent decrease in COD influent concentration greatly reduced power production independent of reactor operation in parallel or serial flow modes. Anode modules connected to two cathodes did not consistently produce more power than the anodes connected to a single cathode, indicating power production became limited by restricted anode performance at low CODs. Cyclic voltammetry and electrochemical impedance spectroscopy data supported restricted anode performance with low COD. These results demonstrate that maintaining power production of MFC stack requires higher influent and effluent COD concentrations. However, overall performance of the MFC in terms of COD removal was not affected by operational modes.

© 2016 Elsevier Ltd. All rights reserved.

## 1. Introduction

Microbial fuel cells (MFCs) can be used to simultaneously remove organic matter from domestic and industrial wastewaters

for electricity production (Arends and Verstraete, 2012; Liu et al., 2004; Pant et al., 2010). In MFCs, organic pollutants are oxidized to  $\text{CO}_2$  by bacteria on the anode chamber, and electrons are transferred from the anode to the cathode where oxygen is reduced to form water (Logan et al., 2006). The potential use of MFCs for wastewater treatment is rapidly advancing (Li et al., 2014; Logan, 2010) through the development of modular structures that have the potential to be implemented at larger scales (Cheng et al., 2014; Feng et al., 2014; Logan et al., 2015; Zhang et al., 2013).

Previous MFC designs that have been used all had limitations in terms of scalability or operability. Cassette designs, where the

\* Corresponding authors. State Key Laboratory of Urban Water Resource and Environment, Harbin Institute of Technology, No. 73 Huanghe Road, Nangang District, Harbin 150090, PR China (Y. Feng). Department of Civil & Environmental Engineering, Penn State University, 231Q Sackett Building, University Park, PA 16802, USA (B.E. Logan).

E-mail addresses: [yujief@hit.edu.cn](mailto:yujief@hit.edu.cn) (Y. Feng), [blogan@psu.edu](mailto:blogan@psu.edu) (B.E. Logan).

anodes are fused to the cathodes, had a compact design but the combined electrodes would be difficult to access and maintain individually (Dekker et al., 2009; Shimoyama et al., 2008). Small tubular systems (~2 L) are not scalable to larger sizes, and thus must be used as many multiple individual reactors (i.e. 96 units to achieve 200 L of reactor volume) (Ge et al., 2015). Stacked plate designs containing a bipolar plate functioning as the anode of one reactor and cathode of an adjacent reactor were subject to voltage reversal (Dekker et al., 2009). Multiple reactors have been separated by an air-drop method (Ieropoulos et al., 2013), overflow (Feng et al., 2014) or thin connecting pipes (Zhuang et al., 2012) between modules to avoid direct hydraulic connections between the units and thus a possible drop due to a direct serial hydraulic connection (Kim et al., 2012), but power densities were low. These indirect hydraulic connections often require additional materials, which could increase the construction costs, water head loss, complexity of the system, and result in a less-compact system. A recent analysis of different reactor designs concluded that the critical factor in scaling up MFCs is maintaining sufficient cathode surface area per volume (cathode specific surface area) as the reactor size is increased in order to achieve rapid COD removal and maintain a good volumetric power density (Logan et al., 2015; Oh et al., 2004).

A modular MFC architecture developed by He et al. (2016) was recently shown to produce one of the highest power densities obtained to date using relatively low-strength domestic wastewater, under continuous flow conditions. The design was based on anode and dual-cathode modules that could individually be placed into or removed from a tank. The approach differed from previous cassette designs as the anodes were not physically bonded to cathodes, and the cathodes were supported by a thin-wire spacer, avoiding cathode deformation caused by hydraulic pressure (He et al., 2014) but allowing good air flow to the cathode surfaces. In a multi-module MFC the anodes and cathodes can be alternated to form a parallel electrode array (Dong et al., 2015; He et al., 2016; Yu et al., 2012). Using a 2-anode, and single dual cathode module, a maximum of  $400 \pm 8 \text{ mW m}^{-2}$  was produced under fed-batch conditions, and 275 and  $300 \text{ mW m}^{-2}$  were achieved under continuous flow conditions. Connecting one anode to two cathodes can increase the volumetric power density, but the approach has only been applied in relatively smaller lab-scale reactors (Kim et al., 2015; Zhang et al., 2011).

Hydraulic connections are particularly important for MFC operation, but they have not been well addressed in most MFC studies. The flow through multiple MFC modules can be made using either serial or parallel flow connections, where flow either enters into only one module and then proceeds to successive modules (serial), or flow enters and exits from each individual module (parallel). Serial flow mode has usually been used for reactors with multiple anodes using a single cathode (Ahn and Logan, 2012), and when connecting many MFC together (Kim et al., 2015; Wang and Han, 2009; Yu et al., 2012). However, some cassette MFC designs have used parallel flow through individual units (Shimoyama et al., 2008). The trade off in these flow designs include: differences in the flow velocities and therefore the hydraulic retention time per module; and the average COD concentration in the modules. In a single MFC with multiple brushes, low COD near the outlet can reduce overall power. When multiple MFCs are connected in series, the low COD concentration in the downstream units can reduce or even eliminate power production compared to those near the inlet (Ahn and Logan, 2013; Ren et al., 2014b). Long-term deprivation of substrate could also result in instability in power generation due to the proliferation of non-exoelectrogenic microorganisms in the biofilm (Miyahara et al., 2013).

In this study, a larger scale (6.1 L) multi-module MFC (4 anode and 3 cathode modules) was examined for power production under

either serial or parallel flow conditions using flow paths that were controlled using baffles. Serial and parallel flow modes were set by either inserting or removing the baffles, with the same net flow applied to the reactor so as to maintain the overall loading rate to the system. The reactor was installed at a municipal wastewater treatment plant and continuously fed domestic wastewater (effluent from a primary clarifier). Operation of the reactor was further examined by either intermittently (every one or two days) alternating the direction of the flow (switching the location for flow entry and exit) or by operating the flow in a fixed, single direction over time.

## 2. Materials and methods

### 2.1. MFC module construction

The MFC module was made of clear polycarbonate with inner dimensions of  $19.5 \text{ cm} \times 25 \text{ cm} \times 12.5 \text{ cm}$  (width  $\times$  length  $\times$  height) (Fig. S1). The influent flowed through porous diffusers made from 20 layers of soft mesh spacers, each with a thickness of 1.5 mm (S1.5, 30PTFE50-625P, Dexmet Corp.), and total thickness of 3 cm, that were used to produce a more uniform cross-sectional flow into the inlet and outlet channels (Fig. S1b). The inlet/outlet channels had a width of 1.5 cm. The MFC contained four anode arrays each containing eight graphite fiber brushes (2.5 cm diameter, 12 cm long; Mill–Rose), and three dual-sided air cathode modules ( $22 \text{ cm} \times 13 \text{ cm} \times 2.5 \text{ cm}$ ) constructed with a gap of 1 cm between the cathodes that was maintained using rigid wire spacers (He et al., 2016) (Fig. 1). Each cathode ( $22 \times 15 \text{ cm}$ ; effective area of  $200 \text{ cm}^2$ ) was made using an activated carbon catalyst and stainless steel current collector using a rolling press method as previously described (Dong et al., 2012a, 2012b). Two cloth separators (46% cellulose and 54% polyester, 0.3 mm thickness, Amplitude Prozorb, Contec Inc., Spartanburg, SC) covered the water side of the AC cathodes to prevent short-circuiting and reduce cathode fouling (Ren et al., 2014a; Zhang et al., 2014a). The first and last anode modules (1 and 4) were connected to only a single cathode, while the inner anode modules (2 and 3) were each connected to two adjacent cathodes (Fig. 1). The anode module and air cathodes formed 6 electrode pairs (Cell 1–6) (Fig. 1b). The anodes 1 and 4 formed Cells 1 and 6 with their matched cathode layer, while the anode 2 formed Cell 2–3 and anode 3 formed Cell 4–5 with the two cathode layers they coupled with. The power generations of the anode modules were obtained by the power obtained from cells formed by each individual anode.

The wastewater was pumped from a storage tank containing primary clarifier overflow into the middle of the reactor by a peristaltic pump (Cole-Parmer, model 7523-90, Masterflex, Vernon Hills, IL), with overflow out of the reactor (Fig. S2a, b) over weirs that were 12.5 cm high (0.5 cm lower than the inner chamber height). Four different flow modes were investigated: two that impacted the hydraulic flow, with serial or parallel through the reactor; and two that impacted flow direction, with flow either fixed in one direction or alternating the entry and exit location by switching them (Table 1). The flow regulation baffles ( $0.5 \text{ cm} \times 1.5 \text{ cm} \times 13 \text{ cm}$ ;  $W \times L \times H$ ) could be removed to hydraulically disconnect one anode module from the others to allow the flow to be simultaneously distributed to each individual module (parallel flow), or be inserted in certain position, to allow flow sequentially through all the anode compartments (serial flow) (Fig. 2). By periodically alternating the location for entry and exit of the flow, the MFC stack could be operated in parallel or serial flow with alternating flow direction, while by fixing the entry and exit of the flow, the MFC stack could be operated in parallel or serial flow with fixed flow direction (Fig. S2, Fig. 2). The total empty bed

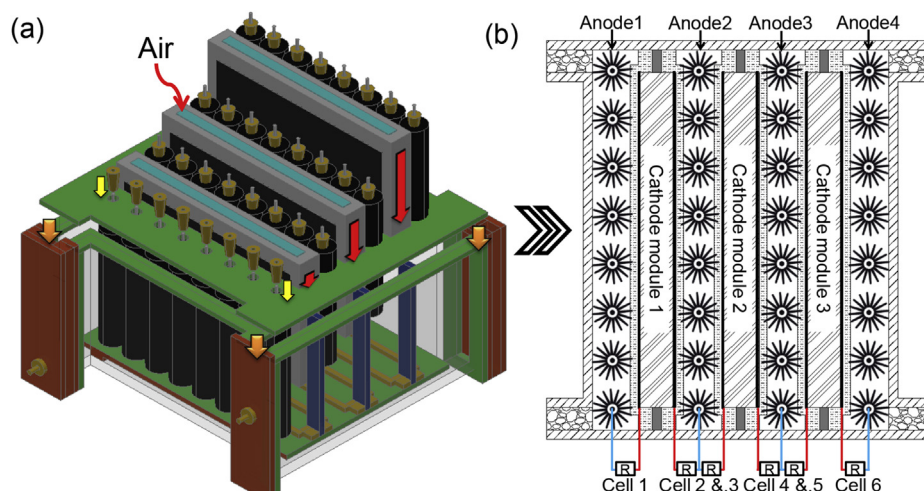


Fig. 1. The schematic of multi-module MFC reactor: (a) isometric view of the MFC stack; (b) top view of electrode arrays.

volume of the reactor was 6.1 L ( $19.5 \text{ cm} \times 25 \text{ cm} \times 12.5 \text{ cm}$ ), with 5.4 L of this volume for installing the electrode modules, and 0.7 L used for the water inlet and outlet channels (Fig. S1a). The liquid volume of a fully assembled reactor was about 4.5 L, producing a cathode specific surface area of  $27 \text{ m}^2 \text{ m}^{-3}$  based on liquid volume, and  $20 \text{ m}^2 \text{ m}^{-3}$  based on total empty bed volume. A cover plate was installed on the top of the modules to hold them in place. The electrode modules were separately accessible and could, therefore, be removed or inserted without disassembling the reactor or removing the cover plate (Fig. 1).

## 2.2. MFC inoculation and operation

The MFC was installed in a basement laboratory at the Pennsylvania State University wastewater treatment plant, and continuously fed with municipal wastewater collected from the primary clarifier that was stored in a 40 L carboy. The hydraulic retention time (HRT) of the total MFC reactor was fixed at 4 h with an influent rate of  $20 \text{ mL min}^{-1}$ . With parallel flow through the different MFC chambers, the average HRT in each module was 4 h, and the flowrate through each module was  $\frac{1}{4}$  of that applied to the reactor, or  $5 \text{ mL min}^{-1}$ . Under serial flow conditions, the flowrate through each module was the same as the applied flowrate ( $20 \text{ mL min}^{-1}$ ) but the HRT of 1 h was  $\frac{1}{4}$  that of the whole reactor HRT. At this overall flowrate and reactor HRT for these two conditions,  $\sim 27 \text{ L}$  of wastewater was used each day, with the remainder of the wastewater returned to the normal treatment plant process train. The chemical oxygen demand (COD) of the wastewater varied from  $\sim 200$  to  $\sim 600 \text{ mg L}^{-1}$ , while the change interval of the soluble chemical oxygen demand (SCOD) was  $100\text{--}300 \text{ mg L}^{-1}$ , over totally 200 days spanning from winter to summer, with generally lower COD concentrations in the summer months. The reactor was operated in a laboratory building (without air conditioning) at the wastewater treatment plant site, with wastewater temperatures determined to be in the range of  $20\text{--}25^\circ \text{C}$ .

The MFC was initially inoculated without cathode modules for 7 days, and refilled daily with fresh wastewater. The MFC stack was then operated in continuous parallel flow mode (Fig. 2) for 12 days (Phase 2, Startup period, Table 1), with the direction of flow alternated in the opposite direction every day to avoid extended exposure of the anodes at the effluent side of the reactor to the lowest COD concentrations. During this period, the external resistance was progressively reduced from open circuit conditions

(OCV) to  $2 \Omega$  (OCV, 2000, 1000, 500, 200, 100, 50, 20, 10, 5 and  $2 \Omega$ ) to gradually acclimate the biofilms to continuous flow conditions and a low external resistance. After this Startup period, the flow direction was periodically alternated every 2 d (days 20–39, Phase 3, Table 1). Days without flow operation (for cathode maintenance, power tests or electrochemical measurements) were not included in this summation of operational days. The reactor was then operated with serial flow (Fig. 2) through the reactor, with alternating flow directions every 2 d (days 40–58, Phase 4). In the last two phases of testing, the flow was set in a fixed direction in parallel (days 59–100, Phase 5) or series (days 101–119, Phase 6) flow through the modules. Flow during Phase 5 was separated and reported as two phases (days 59–79, Phase 5a; and days 80–100, Phase 5b) due to the degradation of cathodes in Phase 5a (Table 1). Electrochemical tests (polarization, cyclic voltammetry and electrochemical impedance spectroscopy measurements) were performed to investigate the impacts of various flow modes on anode performance and overall power generation performance of MFC stack. The electrochemical tests were only conducted when COD concentrations were over  $400 \text{ mg L}^{-1}$  to ensure comparable results between tests (avoiding differences due to changes in COD concentration during tests). After a series of electrochemical tests, the reactor was operated under steady flow conditions for several days to ensure steady conditions for the next flow mode tests.

The cathode was periodically cleaned to minimize changes in performance over time due to cathode fouling. The cathode modules were removed from the reactor and sprayed with a commercial bleaching liquid to disinfect the cathode biofilm. After 5 min, the cathodes were sprayed with dilute hydrochloric acid ( $0.01 \text{ M HCl}$  solution) to dissolve any salts that may have formed on the cathode (Zhang et al., 2014b), and then after 10 min the cathodes were rinsed with tap water before being re-inserted back into the MFC stack. Due to the poor performance of the cathodes even with this cleaning procedure, new cathodes were installed starting on day 80. The additional tests of fixed direction parallel flow (Phase 5b) and tests of fixed direction serial flow (Phase 6) were operated with newly installed cathodes to avoid the impacts of poor cathode performance on these operation periods.

## 2.3. Measurements and analysis

Total COD and SCOD were measured daily using standard methods (COD detector DR 2700, HACH Co., Loveland, CO) and high



**Table 1**  
Operational conditions.

Phase	Days <sup>a</sup>	Operational conditions	Different flow modes		COD (mg L <sup>-1</sup> )
			Flow direction	Hydraulic flow	
1	1–7	Inoculation	No flow	Fed-batch	450 ± 30
2	8–19	Startup	Alternating (1 d)	Parallel	490 ± 70
3	20–39	A-P	Alternating (2 d)	Parallel	480 ± 70
4	40–58	A-S	Alternating (2 d)	Serial	540 ± 85
5a	59–79	F-P	Fixed	Parallel	550 ± 100
5b	80–100	F-P	Fixed	Parallel	350 ± 95
6	101–119	F-S	Fixed	Serial	240 ± 80

<sup>a</sup> Days for cathode maintenance, power tests and electrochemical measurements were not included.

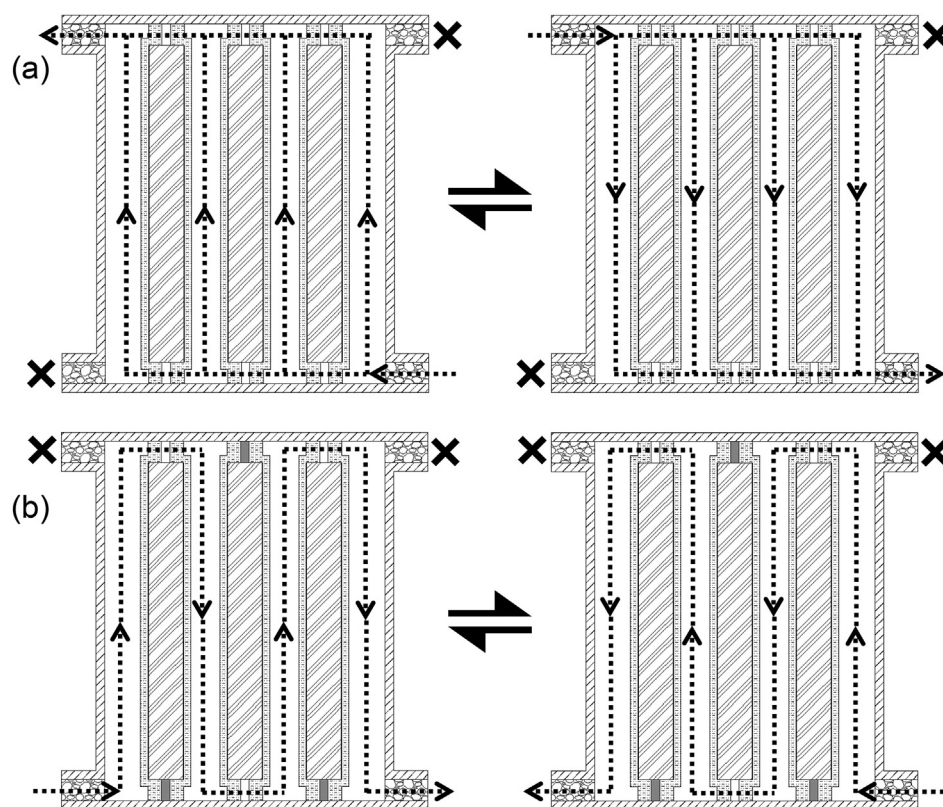


**Fig. 2.** The flow mode regulation by baffles and flow direction alternating by opening or sealing certain outlet end. (a: alternating flow, parallel flow; b: alternating flow, serial flow.)

range (20–1500 mg L<sup>-1</sup>) COD vials using method 5220 (HACH Co.) (APHA, 2005). The SCOD samples were filtered through 0.22 µm pore diameter syringe filters (polyvinylidenedifluoride, PVDF, 25 mm diameter, RESTEK Co.) prior to analysis. Percent removals were calculated each day based on changes in COD and SCOD.

Voltages ( $U$ ) were recorded using a data acquisition system (34972A, Agilent Technologies) at 6 min intervals. Current ( $I=U/R$ ) was calculated based on the resistance ( $R$ ) set using an external resistance box (Model RS-500, 1% precision, Elenco Electronics). The area power density ( $P_d=IU/S$ ) was calculated by normalizing the power using the cathode effective area ( $S$ ) of each cathode (200 cm<sup>2</sup>), while the volumetric power density was based on the total volume ( $v$ ) of the reactor (6.1 L). Polarization and power density tests were performed at the end of each flow mode test by varying the external resistances (1000, 500, 200, 100, 50, 20, 10, 5 and 2 Ω) using a resistor box in single cycle under fed-batch conditions, with 30 or 45 min per resistor. Before each polarization test, the reactor was operated in open circuit for at least 8 h. Polarization tests were conducted under fed-batch conditions to assess

electrode performance under similar COD conditions, except for one test as noted.

Cyclic voltammetry (CV) was conducted using each anode array module as the working electrode, a single cathode as the counter electrode and a Ag/AgCl reference electrode, over a range of  $-0.7$  V  $- +0.1$  V versus a Ag/AgCl electrode (BASi, RE-5B; 210 mV versus a standard hydrogen electrode, SHE) (Zhu et al., 2013). Electrochemical impedance spectroscopy (EIS) was performed to determine the internal resistance of the anode arrays by applying a 10 mV sinusoidal voltage between the electrodes, with a frequency from 100 kHz to 10 mHz (Zhu et al., 2013). The ohmic resistance was defined as the intercept of the high-frequency on the real x-axis value. The non-ohmic resistance, which includes the sum of the charge transfer resistance ( $R_{ct}$ ) and mass diffusion resistance ( $R_d$ ), was determined by fitting a radius to the Nyquist impedance curve (Wu et al., 2015). All electrochemical tests were performed using a potentiostat (BioLogic, VMP3) and associated software (EC-Lab V10.02). Additional supporting calculations can be found in the Supporting Information. The polarization and electrochemical

measurements were conducted at the end of Phases 2, 3, 4, 5b and 6 to reveal the impact of the various operational modes on system performance.

### 3. Results and discussion

#### 3.1. COD removal with different operational modes

During startup (Phase 2), total COD removal with parallel flow operation was  $45 \pm 4\%$ , with  $33 \pm 3\%$  SCOD removal (Fig. 3). In the first series of tests following startup (Phase 3), with the flow still parallel through the modules, but the direction of the flow alternated daily (A-P), COD removals were  $52 \pm 5\%$  for total COD and  $46 \pm 5\%$  for SCOD. When the flow was switched to an alternating direction with a serial flow path (A-S), there was no significant change in total COD or SCOD removal ( $p > 0.05$ , Student's *t*-test; Table S1), with  $52 \pm 6\%$  COD and  $40 \pm 9\%$  SCOD removals. As the wastewater was treated at the same rate (i.e. the flow into four modules in parallel operation was the same as the total flow applied to the entry module for serial flow), this showed that there was no impact in these tests on the percent of COD removal by parallel or serial flow operation, when the flow was alternately switched between exit and entrance points.

The flow was then fixed to always enter the same module. In these fixed direction tests, with parallel flow through the modules (F-P), the percent of COD removal was slightly higher ( $57 \pm 15\%$ ), with a similar SCOD removal ( $43 \pm 21\%$ ) compared to the previous tests. During the final series of tests using a fixed flow direction, with serial flow through all four anode modules (F-S), COD removal was only slightly reduced to  $51 \pm 15\%$ , with a lower SCOD removal of  $35 \pm 10\%$ .

These results for the different operational test conditions showed that there was no significant difference in total COD removal for the different flow directions or serial or parallel flow directions ( $p > 0.05$ , Student's *t*-test; Table S1). For SCOD, the only significant difference among these operational conditions was for the case of parallel and alternating flow conditions (A-P), compared to serial and fixed (F-S) operational conditions ( $p = 0.0024$ ). However, the lack of changes for all other comparisons on COD or SCOD suggested that this difference may have been due more to changes in wastewater characteristics than operational conditions. The wastewater COD concentrations were not significantly different for the two tests with alternating flow (A-P and A-S), but the influent CODs in the last series of tests with fixed flow (F-P and F-S) were significantly different from the first series of tests and from each other (Table S2). For example, for the COD of Phase 3 was  $480 \pm 70 \text{ mg L}^{-1}$  but the averaged COD of Phase 6 was only  $240 \pm 80 \text{ mg L}^{-1}$  (Table 1). These results show that although the COD concentrations changed, the percentage removals of MFC reactor were relatively constant for all four operational modes.

#### 3.2. Power generation with different operational modes

While COD removals were not appreciably affected by reactor operational mode, power production was substantially influenced by reactor operational conditions and wastewater strength. The impact of the operational mode was observed by obtaining polarization data following acclimation of the reactor to the different set conditions.

##### 3.2.1. Power production during startup, Phase 2

During the startup period with continuous flow (day 8–19), the resistance was progressively reduced from OCV to  $2 \Omega$ , while monitoring the anode potentials (Fig. 4a). At the end of Phase 2, anode modules 1 and 4 produced  $290 \pm 8 \text{ mW m}^{-2}$ , and anodes

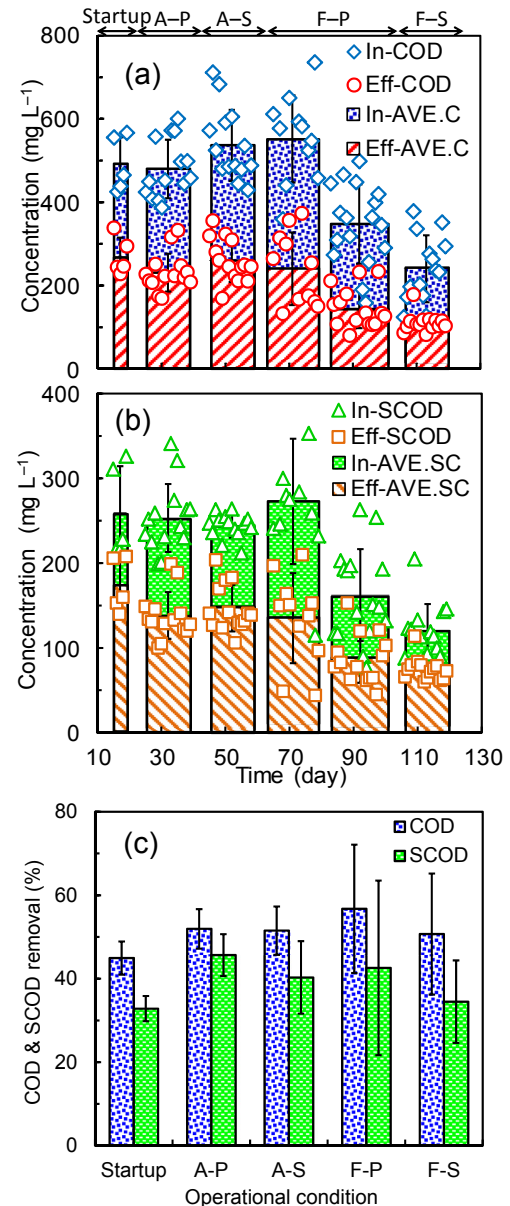


Fig. 3. The COD and SCOD removal with different operation and flow conditions. (In = influent, Eff = effluent, AVE = average, C = total COD or COD, SCOD = soluble COD. Flow modes: Startup = startup period; A-P = alternating direction, parallel flow; A-S = alternating direction, serial flow; F-P = fixed direction, parallel flow; F-S = fixed direction, serial flow.)

modules 2 and 3 generated  $225 \pm 8 \text{ mW m}^{-2}$  (Fig. 4b). Because the power densities were normalized to cathode area, anode modules 2 and 3 actually produced 67% more total power density (connected to 2 cathodes) after Phase 2 than anodes 1 and 4 (connected to one cathode), as the power densities were normalized to twice as much cathode area for modules 2 and 3 compared to modules 1 and 4. On a volumetric power basis, anodes 2 and 3 produced  $5.9 \pm 0.2 \text{ W m}^{-3}$ , compared to  $3.8 \pm 0.1 \text{ W m}^{-3}$  for anodes 1 and 4 (volume for each anode array is assumed to be 1/4 of the total reactor volume of 6.1 L). The overall volumetric power density for this system after Phase 2 with an alternating feed time of 1 d was  $4.8 \text{ W m}^{-3}$  under fed-batch conditions (Fig. S3), compared to the average overall volumetric power density of  $6.1 \pm 0.2 \text{ W m}^{-3}$  under  $20 \Omega$  in continuous flow conditions (Fig. 5a, b). The highest

coulombic efficiency of 28% was obtained at the external resistance of  $2\ \Omega$  (Fig. S4).

### 3.2.2. Alternating flow, parallel direction (A-P), Phase 3

Following the startup period, the MFC was operated in parallel flow mode with an alternating flow direction (A-P, Phase 3, Table 1) every 2 days. For these tests and all subsequent tests, the MFCs were operated at fixed external resistance of  $20\ \Omega$  for maximum power output, which was the resistance that produced the maximum power density in the fed-batch polarization tests following Phase 2. At the end of Phase 3 (A-P), anodes 2 and 3 with two cathodes produced an average power density of  $236 \pm 11\ \text{mW m}^{-2}$ , while anodes 1 and 4 (single cathode) produced  $255 \pm 14\ \text{mW m}^{-2}$  (Fig. 6a). Based on volumetric power, the anode modules connected to two cathodes (anode 2 and 3) produced  $6.2 \pm 0.2\ \text{W m}^{-3}$ , which was 1.9 times that produced by the anodes connected to a single cathode ( $3.3 \pm 0.2\ \text{W m}^{-3}$ , anodes 1 and 4). In this period, the total volumetric power density for whole reactor in fed-batch tests was  $4.8\ \text{W m}^{-3}$  (Fig. 5b, Fig. S3), which was very similar to that obtained during the startup period. The average volumetric power density under continuous flow was  $4.2 \pm 0.5\ \text{W m}^{-3}$  (Fig. 5b). The average coulombic efficiency obtained in Phase 3 under  $20\ \Omega$  was  $8.9 \pm 1.0\%$  (Fig. S4). During the operation in A-P flow mode, the anode arrays with the same combination obtained very uniform power output performance (Fig. S5a).

### 3.2.3. Alternating flow, serial direction (A-S), Phase 4

The MFC flow direction was next changed to serial flow mode. The power densities following serial flow operation in Phase 4 were only slightly lower than those obtained in parallel flow operation (Phase 3), suggesting comparable overall performance under parallel or serial flow with alternating flow direction (Fig. 5). The average power densities for the anodes with two cathodes were  $216 \pm 22\ \text{mW m}^{-2}$ , compared to  $235 \pm 50\ \text{mW m}^{-2}$  for anodes with single cathodes (Fig. 6b). On a volumetric power basis, anodes 2 and 3 produced  $5.7 \pm 0.5\ \text{W m}^{-3}$ , compared to  $3.1 \pm 0.7\ \text{W m}^{-3}$  for anodes 1 and 4, with an overall fed-batch volumetric power density of  $4.2\ \text{W m}^{-3}$  (Fig. 5b). Under continuous flow conditions, the average volumetric power density was  $3.9 \pm 0.5\ \text{W m}^{-3}$ . The key reason for the slightly lower power densities in Phase 4, compared to Phase 3, was likely reduced performance of the cathodes over time, and not serial versus parallel flow direction (Fig. 5a). The COD concentration was not thought to be a factor as the influent CODs during these tests were not significantly different for the two operational periods (Table S2). The average coulombic efficiency obtained in Phase 4 was  $7.1 \pm 1.3\%$  (Fig. S4). During the operation in A-S flow mode, the differences of the performance between anode arrays with the same combination slightly increased compared with the A-P flow mode (Fig. S5b).

### 3.2.4. Fixed flow, parallel direction (F-P), Phase 5

The reactor was next operated in a fixed direction parallel flow with a fixed entry near Anode 4 and exit near Anode 1. The performance of the reactor in this operational mode was divided into two periods due to a significant decrease in average COD concentration from  $550 \pm 100\ \text{mg L}^{-1}$  (Phase 5a) to  $350 \pm 95\ \text{mg L}^{-1}$  (Phase 5b), with an average of  $430 \pm 140\ \text{mg L}^{-1}$  over the complete Phase 5 compared to  $540 \pm 85\ \text{mg L}^{-1}$  in the previous tests (Table 1). From Phase 5a, the power output gradually declined, with an overall average power density under continuous flow for this period of only  $1.1 \pm 0.6\ \text{W m}^{-3}$  (Fig. 5a). Possible reasons for this lower power density compared to previous tests include: cathode degradation; a lower influent COD which would reduce power production (Zhang et al., 2015); or the operational flow direction (fixed versus

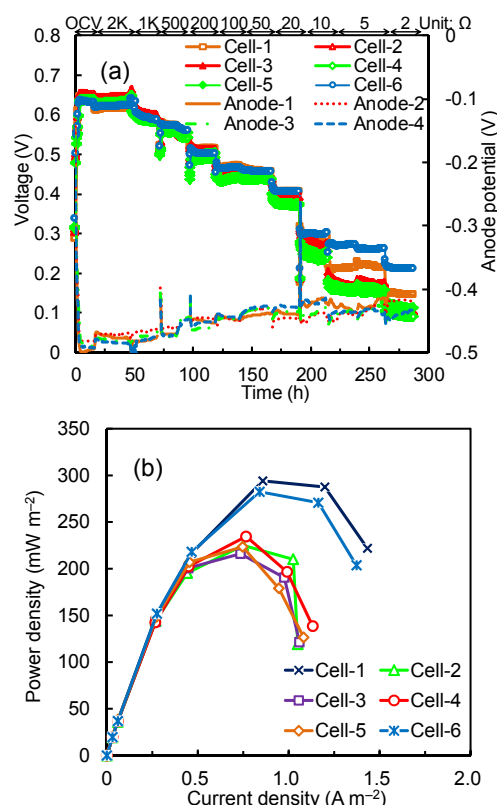
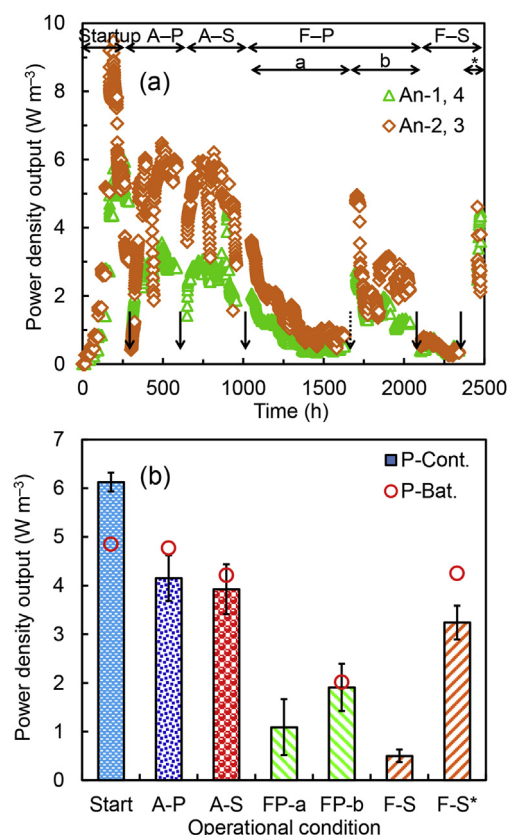


Fig. 4. (a) Voltage and anode potentials during the startup period, and (b) power density curves (fed-batch mode) of the MFC cells at the end of startup period. (Fed-batch mode tests were conducted with COD >  $400\ \text{mg L}^{-1}$ ).

alternating flow). Of these, cathode degradation was suspected to be the main reason for the decline in power, as the COD concentration was similar Phase 5a compared to the previous days of operation. The average coulombic efficiency in Phase 5a was  $3.5 \pm 1.5\%$ , which was also relatively lower than the previous flow mode tests (Phase 3 and 4, Fig. S4). Therefore, new cathodes were installed for data collected in Phase 5b. However, after cathode replacement the COD concentrations in the wastewater sharply decreased (Fig. 3a), as did the power production (Fig. 5a), making it difficult to separate the impact of these different factors on reactor performance.

To try to account for the impact of the change in COD, polarization tests were conducted following Phase 5b using a wastewater sample with a COD above  $400\ \text{mg L}^{-1}$ , which was thought to be sufficiently high to avoid differences in power generation due to low COD concentration of the wastewater. In these fed-batch polarization tests, the overall volumetric power density was only  $2.0\ \text{W m}^{-3}$  (Fig. 5b). The anodes combined with two cathodes generated an average power density of  $105 \pm 25\ \text{mW m}^{-2}$  ( $2.8 \pm 0.2\ \text{W m}^{-3}$ ), while the anodes connected to only one cathode produced  $97 \pm 10\ \text{mW m}^{-2}$  ( $1.3 \pm 0.1\ \text{W m}^{-3}$ ) (Fig. 6c). Therefore, the use of a higher COD concentration could not immediately restore performance to its previous normal level ( $4.8\ \text{W m}^{-3}$  in A-P;  $4.2\ \text{W m}^{-3}$  in A-S). The poorer performance could have been due to fixed flow operation compared to that under alternating flow conditions, or a combination of the fixed flow direction and parallel flow operation. In Phase 5b, the low strength influent wastewater was distributed to four parallel anode modules. Therefore, all the modules were acclimated with low COD. The sustained operation of the reactor under low COD conditions impaired the performance of the four anode arrays in these short-term tests with the higher COD





**Fig. 5.** (a) Volumetric power densities produced by the MFC stack over time. (b) Comparison of the average power densities in continuous flow (P-Cont.) with the maximum power densities obtained under fed-batch conditions after each continuous flow mode phase ended (P-Bat.). (Solid arrows indicate cathode cleaning; dashed arrows show cathodes replacement. Flow modes: Startup = startup period, Phase 2; A-P = alternating direction, parallel flow, Phase 3; A-S = alternating direction, serial flow, Phase 4; F-P = fixed direction, parallel flow, Phase 5a, b; F-S = fixed direction, serial flow, Phase 6; F-S\* = a short fixed direction, serial flow test before fed-batch mode electrochemical tests of F-S tests with COD >400  $\text{mg L}^{-1}$ ).

concentration wastewater (Fig. 6c). The average coulombic efficiency in Phase 5b, however, was  $7.1 \pm 2.2\%$ , which was similar with that of Phase 4 (Fig. S4). During the operation in F-P flow mode, the performance between anodes 2 and 3 was very similar, while anode 1 (near exit) obtained lower performance compared with anode 4 (near entry) (Fig. S5c).

### 3.2.5. Fixed flow, serial direction (F-S), Phase 6

For the final period of operation (Phase 6), the MFC was operated with a fixed flow direction, but with flow through the modules in series (Fig. 1). The entry was fixed near Anode 1, while the exit near anode 4. The average influent COD concentration during this period was only  $240 \pm 80 \text{ mg L}^{-1}$ , which was likely the reason for the low overall power output under continuous flow conditions of  $0.45 \pm 0.10 \text{ W m}^{-3}$  (Fig. 5b). Polarization tests following this F-S mode operation were conducted using wastewater that had a COD above  $400 \text{ mg L}^{-1}$ , in order to better compare reactor performance to previous tests. With this higher COD concentration, the power output in continuous flow mode ( $20 \Omega$ ) reached  $3.3 \pm 0.4 \text{ W m}^{-3}$  (Fig. 5a, b), which was close to maximum power densities obtained in previous tests in Phases 3 ( $4.2 \pm 0.5 \text{ W m}^{-3}$ ) and 4 ( $3.9 \pm 0.5 \text{ W m}^{-3}$ ). This confirmed that the low power density during the F-S operational period was primarily due to the low COD concentration. The average coulombic efficiency in Phase 6 ( $9.4 \pm 6.0\%$ ) was the highest among the flow mode tests (Phase

3–6) (Fig. S4). The greater standard deviation was due to fluctuations in the concentration of COD in the influent. The occasional increase in the COD, however, was not sufficient to produce a recovery of overall power (Fig. 3, Fig. S4).

In Phase 6, the influent COD concentration was very low, and only slightly higher than the  $\sim 150\text{--}200 \text{ mg/L}$  previously shown to greatly reduce current generation with a filtered domestic wastewater fed single anode reactor in batch mode tests (Zhang et al., 2015), and  $\sim 250 \text{ mg/L}$  that started to reduce current production and increase internal resistance by a brush anodes multi-electrode MFCs (He et al., 2016). The upstream modules were acclimated to fresh influent wastewater with a higher COD, but the downstream anodes were exposed to much lower CODs. As a result of these different conditions, the first two anode modules 1 and 2 produced power densities comparable to that obtained in Phase 2–4 (Fig. 6, Fig. 7). However, the two downstream anode modules 3 and 4 had much lower maximum power densities in Phase 6. The lower performance of downstream anode performance was also observed under continuous flow conditions (Fig. S5d).

### 3.3. Electrochemical tests

Cyclic Voltammetry (CV) was used to examine the inherent performance of the cathodes when operated under the different operational conditions (Fig. S6a). In general, the maximum current densities produced in CV tests by anodes connected to two cathodes was larger than those obtained for the anodes connected to a single cathode, consistent with polarization data showing the same trend for maximum power densities (Fig. 7). For example, following startup, anodes 2 and 3 connected to two cathodes had a higher maximum current in the CV tests ( $74 \pm 20 \text{ mA}$ ) than the anodes 1 and 4 that were connected to a single cathode ( $41 \pm 17 \text{ mA}$ ). However, the changes in CV maximum current densities were more variable than the maximum power densities based on polarization data. In alternating flow tests (A-P and A-S), the electron transfer capacity of the anodes based on CV results showed further improvement, with anodes 2 and 3 reaching  $133 \pm 6 \text{ mA}$ , and anodes 1 and 4 increasing to  $87 \pm 9 \text{ mA}$ . However, the power densities for anodes 2 and 3 based on polarization tests were quite similar in all three conditions (startup, A-P and A-S) (Fig. 7, Fig. S6). This improved performance based on CV tests suggests that alternating the flow may have improved the capacity of the anodes for greater current and power generation, but increased power could not be obtained likely due to power densities limited by the cathode.

In the subsequent tests with the fixed direction flow tests (F-P and F-A), maximum currents obtained for the anodes in CV tests decreased (Fig. 7, Fig. S6). This decrease was likely due more to the low COD concentrations during this period than the fixed flow direction operation as the power densities in polarization tests also decreased. In addition, the maximum current densities of the anodes connected to two cathodes (anodes 2 and 3) were not consistently larger than those connected to single cathodes (anodes 1 and 4). Thus, a combination of the flow direction and low COD concentrations did not result in definite trends in performance other than the observation that there was a general decrease in anode performance during the fixed direction tests with low influent COD concentrations.

Analysis of the internal resistance of the anode configurations over time using EIS generally showed trends similar to those obtained using CV tests, as the anodes connected to two cathodes had lower internal resistances than anodes connected to single cathodes (Fig. 8, Fig. S7). In the startup period, the internal resistances of anodes connected to two cathodes were  $6.4 \pm 3.0 \Omega$ , which was lower than that obtained for anodes connected to a single cathode ( $8.7 \pm 3.3 \Omega$ ). For the A-P alternating flow direction tests, the anode

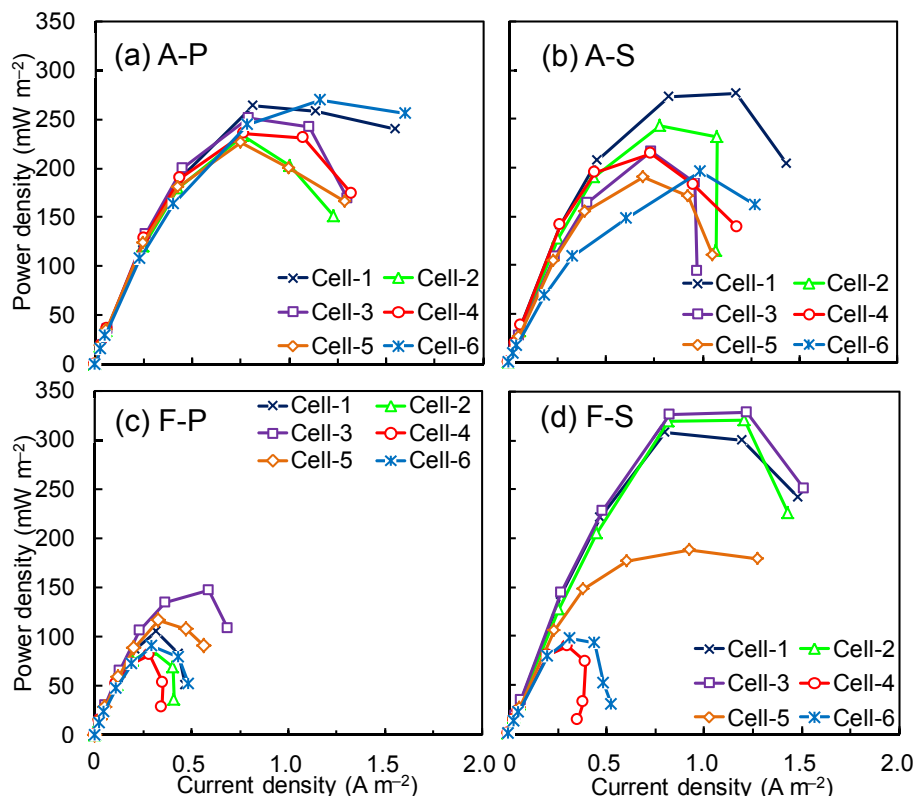


**Fig. 6.** Power density curves for the power generation of multi-module MFC following operation under various continuous flow modes: (a) alternating direction, parallel flow, A-P, Phase 3; (b) alternating direction, serial flow, A-S, Phase 4; (c) fixed direction, parallel flow, F-P, Phase 5b; (d) fixed direction, serial flow, F-S, Phase 6. (All tests were obtained under fed-batch conditions with COD > 400 mg L<sup>-1</sup>).

resistances further decreased to  $1.3 \pm 0.1 \Omega$  (anodes with two cathodes) and  $3.0 \pm 1.8 \Omega$  (anodes with one cathode), and remained low for the A-S phase. These decreases in internal resistance were consistent with higher current densities in CV tests. However, in the fixed flow F-P tests, the internal resistance remained low ( $2.4 \pm 1.1 \Omega$  for anodes 2 and 3;  $2.5 \pm 0.2 \Omega$  for anodes 1 and 4), suggesting the anodes could have produced higher current or power. However, the CV results showed no increase in current. As low COD conditions persisted ( $240 \pm 80 \text{ mg L}^{-1}$  COD) in the F-S phase, the anode internal resistances increased to  $9.9 \pm 1.3 \Omega$  for anodes

with two cathodes, and  $9.4 \pm 1.6 \Omega$  for anodes with one cathode. Thus, at these low CODs, power, current, and internal resistance of the anodes were more critical than the performance of the cathode due to the very low strength of the wastewater (Fig. S7, Fig. S8, Table S3).

#### 3.4. Overall assessment of operational conditions on power generation

Power generation by MFCs has usually been considered to be limited by the cathode, based on tests using high concentrations of acetate, industrial wastewaters or domestic wastewater (Logan et al., 2015; Oh et al., 2004). However, the results obtained in this study demonstrate that the anode can be the main factor in MFC performance at low COD concentrations. When the anodes were connected to two cathodes, and the COD concentration of the wastewater entering the MFCs was relatively high ( $\sim 500 \text{ mg L}^{-1}$ ), power production was higher ( $6.0 \pm 0.5 \text{ W m}^{-3}$  for anode 2, and  $5.8 \pm 0.5 \text{ W m}^{-3}$  for anode 3) than power densities obtained with anodes connected to single cathodes ( $3.6 \pm 0.2 \text{ W m}^{-3}$  for anode 1 and  $3.2 \pm 0.5 \text{ W m}^{-3}$  for anode 4) (Fig. 7). These results are consistent with previous findings that increasing the cathode area per volume of reactor can increase power per area of anode and volumetric power density (Cheng and Logan, 2011; Fan et al., 2012; Kim et al., 2015; Oh et al., 2004; Zhang et al., 2011). In the cathode-limited operational conditions, coupling two cathodes together increased current and power generation from a single anode array, which resulted in positive effects on the anode performances in term of maximum current output in CV tests (Fig. 7) and the internal resistances (Fig. 8). However, when the influent COD concentrations became much lower, as they did in the later fixed flow

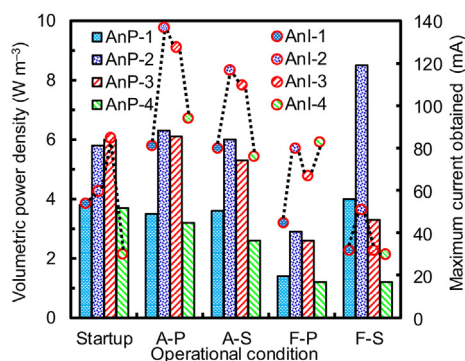


**Fig. 7.** The maximum volumetric power density in polarization tests and maximum current in CV tests generated by four anode modules under various flow modes. (An = anode, P = power, I = current; Flow modes: Startup = startup period, Phase 2; A-P = alternating direction, parallel flow, Phase 3; A-S = alternating direction, serial flow, Phase 4; F-P = fixed direction, parallel flow, Phase 5b; F-S = fixed direction, serial flow, Phase 6; all tests under fed-batch conditions).



tests (Phase 6, average influent CODs of  $240 \text{ mg L}^{-1}$ ), anodes with two cathodes did not consistently produce more power than anodes connected to a single cathode (Fig. 7, Fig. S6d). This signaled a shift from cathode-limited performance to anode-limited performance. In this condition, the positive feedback of coupling two cathodes for an anode array was eliminated due to the low COD concentration, which adversely impacted power production. To avoid anode-limited performance, and to maintain higher power densities, the MFC should be operated with higher influent and effluent CODs so that the electrode is not operated for extended periods with wastewater at a low COD. Water quality needed for discharge in terms of a much lower COD can be obtained using a secondary process, such as an anaerobic fluidized bed membrane bioreactor, as previously demonstrated (Ren et al., 2014a).

Low COD concentrations in MFCs did not impact the percentage of COD removed in the reactor, but they did affect reactor stability and performance in terms of power production. The percentage of COD removed was relatively unaffected by the different operational conditions (serial or parallel, alternating or fixed flow) with no clear pattern associated with these conditions (Fig. 3). With alternating flow, either in serial or parallel flow conditions, power production was very stable with the high influent COD concentrations, suggesting little difference due to serial or parallel flow conditions. The impact of fixed flow operation compared to alternating flow, however, was inconclusive due to the low COD concentrations in the fixed flow tests. Initial tests with fixed flow at high COD concentrations (F-Pa) showed a decrease in performance even with high COD, due to deterioration of cathode performance. However, a change in the COD from high to low concentrations did not permit direct comparisons of alternating and fixed flow conditions based only on power. Electrochemical tests using EIS showed an increase in internal resistance during operation in fixed flow conditions with serial flow, but CV results showed the opposite trend. Continued operation of the MFC under low COD concentrations, therefore, precluded determination of the impact of the operational condition on performance.

For the practical operation of a pilot multi-module MFC stack, parallel flow with alternating flow direction may be the best choice to avoid the lower power output in some modules that could occur due to an imbalance in COD concentrations within the different modules. Matching one anode array with an additional cathode will

also be useful for improving anode performance and increasing overall power generation. The outer anode banks (first and last) could likely be constrained to always having a single cathode, but as additional anode banks are added, for example having 100 anode arrays as opposed to 4 here, the impact of these outer anode arrays on overall power production would be relatively limited.

#### 4. Conclusions

A scaled up multi-module MFC stack operated with different flow directions and electrode combinations was operated at a treatment plant under highly variable influent COD concentrations. With an alternating flow direction, power generation was relatively uniform between modules operated in either parallel or serial flow, with power densities of  $4.8 \text{ W m}^{-3}$  with parallel flow, and  $4.2 \text{ W m}^{-3}$  for serial flow. Anodes connected to two cathodes generated 1.9 times more power than anodes connected to a single cathode, under these alternating flow conditions with a COD of  $\sim 500 \text{ mg L}^{-1}$ , demonstrating cathode-limited performance. Low COD concentrations reduced performance in the fixed direction tests, but there was no general trend that could establish the decrease in performance solely to the flow direction. When the COD concentrations were very low, power generation became limited by the low COD concentrations due to impaired anode performance. The flow modes influenced module performance primarily by producing low COD concentration in certain modules based on the operation mode. However, no significant differences were obtained in COD removal due to the different flow modes or fluctuations in influent COD. These results demonstrate successful treatment of domestic wastewater in a larger-scale MFC, and document the importance of higher influent and effluent CODs for maintaining power production. Effluent quality needed for wastewater discharge will need to be obtained using a secondary polishing step.

#### Acknowledgements

The authors thank David Jones for help with the manufacture of the reactor and analytical measurements. This research was supported by the Strategic Environmental Research and Development Program (SERDP), Award KUS-I1-003-13 from the King Abdullah University of Science and Technology (KAUST), the National Natural Science Fund for Distinguished Young Scholars (Grant No. 51125033), the International Cooperating Project between China and European Union (Grant No. 2014DFE90110), National Natural Science Foundation of China (Grant No. 51408336, to X.Z.), and a scholarship (No. 201206120191) to W.H. from the China Scholarship Council (CSC).

#### Appendix A. Supplementary data

Supplementary data related to this article can be found at <http://dx.doi.org/10.1016/j.watres.2016.09.008>.

#### References

- Ahn, Y., Logan, B.E., 2012. A multi-electrode continuous flow microbial fuel cell with separator electrode assembly design. *Appl. Microbiol. Biotechnol.* 93 (5), 2241–2248.
- Ahn, Y., Logan, B.E., 2013. Domestic wastewater treatment using multi-electrode continuous flow MFCs with a separator electrode assembly design. *Appl. Microbiol. Biotechnol.* 97 (1), 409–416.
- APHA, 2005. Standard Methods for the Examination of Water and Wastewater. American Public Health Association, American Water Works Association, Water Environment Federation, Washington, DC.
- Arends, J.B.A., Verstraete, W., 2012. 100 years of microbial electricity production: three concepts for the future. *Microb. Biotechnol.* 5 (3), 333–346.

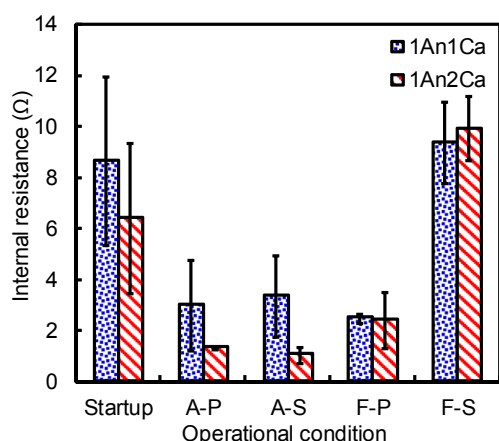


**Fig. 8.** Comparison of total internal resistances of anode modules based on EIS analysis with different flow and operational conditions. (Flow modes: Startup = startup period, Phase 2; A-P = alternating direction, parallel flow, Phase 3; A-S = alternating direction, serial flow, Phase 4; F-P = fixed direction, parallel flow, Phase 5b; F-S = fixed direction, serial flow, Phase 6; 1An1Ca = 1 anode module with 1 cathode; 1An2Ca = 1 anode module with two cathodes; all tests under fed-batch conditions).

- Cheng, S.A., Logan, B.E., 2011. Increasing power generation for scaling up single-chamber air cathode microbial fuel cells. *Bioresour. Technol.* 102 (6), 4468–4473.
- Cheng, S.A., Ye, Y.L., Ding, W.J., Pan, B., 2014. Enhancing power generation of scale-up microbial fuel cells by optimizing the leading-out terminal of anode. *J. Power Sources* 248, 931–938.
- Dekker, A., Ter Heijne, A., Saakes, M., Hamelers, H.V.M., Buisman, C.J.N., 2009. Analysis and improvement of a scaled-up and stacked microbial fuel cell. *Environ. Sci. Technol.* 43 (23), 9038–9042.
- Dong, H., Yu, H., Wang, X., 2012a. Catalysis kinetics and porous analysis of rolling activated carbon-PTFE air-cathode in microbial fuel cells. *Environ. Sci. Technol.* 46 (23), 13009–13015.
- Dong, H., Yu, H., Wang, X., Zhou, Q., Feng, J., 2012b. A novel structure of scalable air-cathode without Nafion and Pt by rolling activated carbon and PTFE as catalyst layer in microbial fuel cells. *Water Res.* 46 (17), 5777–5787.
- Dong, Y., Qu, Y.P., He, W.H., Du, Y., Liu, J., Han, X.Y., Feng, Y.J., 2015. A 90-liter stackable baffled microbial fuel cell for brewery wastewater treatment based on energy self-sufficient mode. *Bioresour. Technol.* 195, 66–72.
- Fan, Y.Z., Han, S.K., Hong, L., 2012. Improved performance of CEA microbial fuel cells with increased reactor size. *Energy Environ. Sci.* 5 (8), 8273–8280.
- Feng, Y.J., He, W.H., Liu, J., Wang, X., Qu, Y.P., Ren, N.Q., 2014. A horizontal plug flow and stackable pilot microbial fuel cell for municipal wastewater treatment. *Bioresour. Technol.* 156, 132–138.
- Ge, Z., Wu, L., Zhang, F., He, Z., 2015. Energy extraction from a large-scale microbial fuel cell system treating municipal wastewater. *J. Power Sources* 297, 260–264.
- He, W.H., Liu, J., Li, D., Wang, H.M., Qu, Y.P., Wang, X., Feng, Y.J., 2014. The electrochemical behavior of three air cathodes for microbial electrochemical system (MES) under meter scale water pressure. *J. Power Sources* 267, 219–226.
- He, W.H., Zhang, X.Y., Liu, J., Zhu, X.P., Feng, Y.J., Logan, B.E., 2016. Microbial fuel cells with an integrated spacer and separate anode and cathode modules. *Environ. Sci. Water Res. Technol.* 2, 186–195.
- Ieropoulos, I.A., Ledezma, P., Stinchcombe, A., Papaharalabos, G., Melhuish, C., Greenman, J., 2013. Waste to real energy: the first MFC powered mobile phone. *Phys. Chem. Chem. Phys.* 15 (37), 15312–15316.
- Kim, D., An, J., Kim, B., Jang, J.K., Kim, B.H., Chang, I.S., 2012. Scaling-up microbial fuel cells: configuration and potential drop phenomenon at series connection of unit cells in shared anolyte. *ChemSusChem* 5 (6), 1086–1091.
- Kim, K.Y., Yang, W., Logan, B.E., 2015. Impact of electrode configurations on retention time and domestic wastewater treatment efficiency using microbial fuel cells. *Water Res.* 80, 41–46.
- Li, W.W., Yu, H.Q., He, Z., 2014. Towards sustainable wastewater treatment by using microbial fuel cells-centered technologies. *Energy Environ. Sci.* 7 (3), 911–924.
- Liu, H., Ramnarayanan, R., Logan, B.E., 2004. Production of electricity during wastewater treatment using a single chamber microbial fuel cell. *Environ. Sci. Technol.* 38 (7), 2281–2285.
- Logan, B.E., 2010. Scaling up microbial fuel cells and other bioelectrochemical systems. *Appl. Microbiol. Biotechnol.* 85 (6), 1665–1671.
- Logan, B.E., Hamelers, B., Rozendal, R.A., Schröder, U., Keller, J., Freguia, S., Aelterman, P., Verstraete, W., Rabaey, K., 2006. Microbial fuel cells: methodology and technology. *Environ. Sci. Technol.* 40 (17), 5181–5192.
- Logan, B.E., Wallack, M.J., Kim, K.Y., He, W.H., Feng, Y.J., Saikaly, P.E., 2015. Assessment of microbial fuel cell configurations and power densities. *Environ. Sci. Technol. Lett.* 2 (8), 206–214.
- Miyahara, M., Hashimoto, K., Watanabe, K., 2013. Use of cassette-electrode microbial fuel cell for wastewater treatment. *J. Biosci. Bioeng.* 115 (2), 176–181.
- Oh, S., Min, B., Logan, B.E., 2004. Cathode performance as a factor in electricity generation in microbial fuel cells. *Environ. Sci. Technol.* 38 (18), 4900–4904.
- Pant, D., Van Bogaert, G., Diels, L., Vanbroekhoven, K., 2010. A review of the substrates used in microbial fuel cells (MFCs) for sustainable energy production. *Bioresour. Technol.* 101 (6), 1533–1543.
- Ren, L.J., Ahn, Y., Logan, B.E., 2014a. A two-stage microbial fuel cell and anaerobic fluidized bed membrane bioreactor (MFC-AFMBR) system for effective domestic wastewater treatment. *Environ. Sci. Technol.* 48 (7), 4199–4206.
- Ren, L.J., Zhang, X.Y., He, W.H., Logan, B.E., 2014b. High current densities enable exoelectrogens to outcompete aerobic heterotrophs for substrate. *Biotechnol. Bioeng.* 111 (11), 2163–2169.
- Shimoyama, T., Komukai, S., Yamazawa, A., Ueno, Y., Logan, B.E., Watanabe, K., 2008. Electricity generation from model organic wastewater in a cassette-electrode microbial fuel cell. *Appl. Microbiol. Biotechnol.* 80 (2), 325–330.
- Wang, B., Han, J.L., 2009. A single chamber stackable microbial fuel cell with air cathode. *Biotechnol. Lett.* 31 (3), 387–393.
- Wu, S.J., Liang, P., Zhang, C.Y., Li, H., Zuo, K.C., Huang, X., 2015. Enhanced performance of microbial fuel cell at low substrate concentrations by adsorptive anode. *Electrochim. Acta* 161, 245–251.
- Yu, J., Seon, J., Park, Y., Cho, S., Lee, T., 2012. Electricity generation and microbial community in a submerged-exchangeable microbial fuel cell system for low-strength domestic wastewater treatment. *Bioresour. Technol.* 117, 172–179.
- Zhang, F., Ahn, Y., Logan, B.E., 2014a. Treating refinery wastewaters in microbial fuel cells using separator electrode assembly or spaced electrode configurations. *Bioresour. Technol.* 152 (1), 46–52.
- Zhang, F., Ge, Z., Grimaud, J., Hurst, J., He, Z., 2013. Long-term performance of liter-scale microbial fuel cells treating primary effluent installed in a municipal wastewater treatment facility. *Environ. Sci. Technol.* 47 (9), 4941–4948.
- Zhang, X.Y., Cheng, S.A., Liang, P., Huang, X., Logan, B.E., 2011. Scalable air cathode microbial fuel cells using glass fiber separators, plastic mesh supporters, and graphite fiber brush anodes. *Bioresour. Technol.* 102 (1), 372–375.
- Zhang, X.Y., He, W.H., Ren, L.J., Stager, J., Evans, P.J., Logan, B.E., 2015. COD removal characteristics in air-cathode microbial fuel cells. *Bioresour. Technol.* 176, 23–31.
- Zhang, X.Y., Pant, D., Zhang, F., Liu, J., He, W.H., Logan, B.E., 2014b. Long-term performance of chemically and physically modified activated carbons in air cathodes of microbial fuel cells. *ChemElectroChem* 1 (11), 1859–1866.
- Zhu, X.P., Tokash, J.C., Hong, Y.Y., Logan, B.E., 2013. Controlling the occurrence of power overshoot by adapting microbial fuel cells to high anode potentials. *Bioelectrochemistry* 90, 30–35.
- Zhuang, L., Yuan, Y., Wang, Y., Zhou, S., 2012. Long-term evaluation of a 10-liter serpentine-type microbial fuel cell stack treating brewery wastewater. *Bioresour. Technol.* 123, 406–412.